PERGAMON

www.elsevier.nl/locate/poly

Polyhedron 19 (2000) 1193–1203

POLYHEDRON

Axial ligand substitution and photoisomerization reactions in ruthenium(II) *trans* mixed-chelate complexes containing the ligands 1,2-phenylenebis(dimethylarsine) and 2,2′-bipyridine or 1,10-phenanthroline

Benjamin J. Coe [a,*], Christopher I. McDonald [a], Samantha M. Couchman [b], John C. Jeffery [b], Leigh H. Rees [b], Simon J. Coles [c], Thomas Gelbrich [c], Michael B. Hursthouse [c]

[a] *Department of Chemistry, University of Manchester, Oxford Road, Manchester M13 9PL, UK*
[b] *Department of Chemistry, University of Bristol, Cantock's Close, Bristol BS8 1TS, UK*
[c] *EPSRC X-ray Crystallography Service, Department of Chemistry, University of Southampton, Highfield, Southampton SO17 1BJ, UK*

Received 28 January 2000; accepted 25 February 2000

Abstract

The nitrosyl complex in *trans*-[RuCl(pdma)(bpy)(NO)][PF_6]$_2$ (pdma = 1,2-phenylenebis(dimethylarsine), bpy = 2,2′-bipyridine) reacts at room temperature with stoichiometric NaN_3, followed by an excess of a neutral ligand L_1 in 2-butanone under reflux, to afford high yields of the mono-substituted derivatives *trans*-[RuCl(pdma)(bpy)L_1]PF_6 (L_1 = pyridine (py) **1**, triphenylphosphine (PPh_3) **2**, *N*-methylimidazole (mim) **3**, acetonitrile (MeCN) **4**, dimethylsulfoxide (dmso) **5** or pyrazine (pyz) **6**). The related compound *trans*-[RuCl(pdma)(phen)(NO)][PF_6]$_2$ (phen = 1,10-phenanthroline) reacts similarly to yield *trans*-[RuCl(pdma)(phen)L_1]PF_6 (L_1 = py **8**, PPh_3 **9**, mim **10** or pyz **11**). The pyrazine complexes in **6** and **11** react with MeI at room temperature in acetone to afford *trans*-[RuCl(pdma)(L–L)(mpyz$^+$)][PF_6]$_2$ (mpyz$^+$ = *N*-methylpyrazinium, L–L = bpy **7** or phen **12**, respectively). **3** reacts with an excess of a neutral ligand L_2 in the presence of stoichiometric $AgCF_3CO_2$ in water/acetone under reflux to afford high yields of the di-substituted derivatives *trans*-[Ru(pdma)(bpy)mim(L_2)][PF_6]$_2$ (L_2 = mim **13**, py **14** or MeCN **15**) and **2** reacts similarly with $AgCF_3CO_2$ in water/MeCN to give *trans*-[RuCl(pdma)(bpy)PPh_3(MeCN)][PF_6]$_2$ (**16**). The complexes in **1**–**16** exhibit intense $d_\pi(Ru^{II}) \rightarrow \pi^*(L–L)$ and $d_\pi(Ru^{II}) \rightarrow \pi^*(L_1/L_2)$ (L_1/L_2 = py, pyz or mpyz$^+$) metal-to-ligand charge-transfer absorption bands in the near-UV–visible region and are mildly photosensitive in solution. Solar irradiation leads to isomerization; for example **3** is converted into *cis*-[RuCl(pdma)(bpy)mim]PF_6 (**17**) over a period of ca. 100 h exposure to diffuse sunlight in acetone. Single crystal X-ray structures have been determined for **1**, **2**·DMF, **3**, **12**·3MeCN, **14**·DMF and **17**.

Keywords: Photoisomerization; Ruthenium

1. Introduction

It has recently become apparent that ruthenium(II) complexes of N-heterocyclic chelating ligands such as 2,2′-bipyridine (bpy), 1,10-phenanthroline (phen) or 2,2′:6′,2″-terpyridine have potential for applications as components of photoactive molecular-level devices [1,2]. Of particular current interest is the discovery that relatives of the prototypical complex $[Ru^{II}(bpy)_3]^{2+}$ can act as efficient sensitizers when covalently attached to the surfaces of semiconducting nanocrystalline metal oxide electrodes in photovoltaic cells [3,4]. The utility of organotransition metal complexes in these and related devices rests upon the fact that photon absorption by metal-to-ligand charge-transfer (MLCT) chromophores can induce sequential, intramolecular electron or energy-transfer processes. The design of potentially useful MLCT-based molecular devices requires optimization of both electronic and stereochemical properties, and a particular emphasis on structurally well defined systems has emerged recently [5–7]. With functionalized octahedral MLCT chromophores, a *trans* disposition of attached donor/acceptor ('quencher') units is likely to be advantageous in order to achieve phenomena such as long-lived charge-separation. One approach to the preparation of such assemblies involves controlled ligand substitutions at *trans* octahedral metal centres.

Although 'chromophore-quencher' complexes based on *trans*-$\{Ru^{II}(bpy)_2\}^{2+}$ centres have been prepared [8], these undergo extremely facile photoinitiated ligand dissociation

* Corresponding author. Tel.: +44-161-275-4601; fax: +44-161-275-4598; e-mail: b.coe@man.ac.uk

0277-5387/00/$ - see front matter
PII S0277-5387(00)00369-7

and isomerization reactions. In attempts to identify alternative systems suitable for the preparation of stable *trans* MLCT chromophoric assemblies, we have chosen to explore the derivative chemistry of ruthenium(II) complexes of the chelating ligand 1,2-phenylenebis(dimethylarsine) (pdma). The precursor *trans*-$[Ru^{II}Cl(pdma)_2(NO)]^{2+}$ [9] readily undergoes nitrosyl substitution reactions to afford mono- and dinuclear derivatives containing the non-chromophoric *trans*-$\{Ru^{II}Cl(pdma)_2\}^+$ core [10,11], but subsequent chloride substitutions are remarkably difficult [10]. We have recently reported the mixed-chelates *trans*-$[Ru^{II}Cl(pdma)(L–L)(NO)]^{2+}$ (L–L = bpy or phen) [12], which were designed to act as versatile synthetic precursors to functionalized *trans* assemblies via stepwise axial ligand substitutions. The reactivity of these complexes and the photostability of the resulting products are the subjects of the present report.

2. Experimental

2.1. Materials and procedures

The compound $RuCl_3 \cdot 2H_2O$ was supplied by Johnson Matthey plc and pdma was obtained from Dr P.G. Edwards, University of Wales College of Cardiff. The salts *trans*-$[RuCl(pdma)(L–L)(NO)][PF_6]_2$ (L–L = bpy or phen) were prepared according to published procedures [12]. All other reagents were obtained commercially and used as supplied. All reactions were conducted under an argon atmosphere. Products were dried overnight at room temperature in a vacuum desiccator ($CaSO_4$) prior to characterization.

2.2. Instrumentation

^{1}H NMR spectra were recorded on a Varian Gemini 200 spectrometer and all shifts are referenced to $SiMe_4$. The complex fine splitting of the pyridine or 2,2′-bipyridine proton resonances is ignored and the signals are reported as simple doublets or triplets. Elemental analyses were performed by the Microanalytical Laboratory, University of Manchester. Infrared spectra were obtained as KBr discs with an ATI Mattson Genesis Series FTIR instrument. FAB mass spectra were recorded using a Kratos Concept spectrometer with a 6–8 keV Xe atom beam and 3-nitrobenzyl alcohol as matrix.

Cyclic voltammetric measurements were carried out using an EG&G PAR model 173 potentiostat/galvanostat with a model 175 universal programmer. A single-compartment cell was used with the saturated calomel reference electrode (SCE) separated by a salt bridge from the platinum-bead working electrode and platinum-wire auxiliary electrode. Acetonitrile (HPLC grade) was used as received and tetra-*n*-butylammonium hexafluorophosphate, twice recrystallized from ethanol and dried in vacuo, was used as supporting electrolyte. Solutions containing ca. 10^{-3} mol dm^{-3} analyte (0.1 mol dm^{-3} electrolyte) were deaerated by purging with N_2. All $E_{1/2}$ values were calculated from $(E_{pa}+E_{pc})/2$ at a scan rate of 200 mV s^{-1}.

2.3. Preparations

2.3.1. *trans*-[RuCl(pdma)(bpy)py]PF_6 (1)

A solution of *trans*-$[RuCl(pdma)(bpy)(NO)][PF_6]_2$ (50 mg, 0.056 mmol) and NaN_3 (3.7 mg, 0.057 mmol) in pyridine (10 cm^3) was stirred at room temperature for 2 h, then heated at reflux for 1 h. Addition of aqueous NH_4PF_6 yielded a deep red precipitate which was filtered off, washed with water and dried. Yield: 39 mg, 87%. *Anal*. Found: C, 37.4; H, 3.65; N, 5.10. Calc. for $C_{25}H_{29}As_2ClF_6N_3PRu$: C, 37.4; H, 3.65; N, 5.25%. ^{1}H NMR (200 MHz, CD_3CN): δ 9.27 (2H, d, J = 5.8 Hz, $H^{6,6'}$), 8.55 (2H, d, J = 8.0 Hz, $H^{3,3'}$), 8.17 (2H, t, $H^{4,4'}$), 8.05 (2H, m, C_6H_2), 7.82 (2H, t, $H^{5,5'}$), 7.73–7.65 (5H, m, $pyH^{2,4,6}$ and C_6H_2), 6.93 (2H, t, $pyH^{3,5}$), 1.78 (6H, s, 2AsMe), 1.62 (6H, s, 2AsMe). *m/z*: 658 ($[M-PF_6^-]^+$) and 579 ($[M-PF_6^- - py]^+$).

2.3.2. *trans*-[RuCl(pdma)(bpy)PPh_3]PF_6 (2)

A solution of *trans*-$[RuCl(pdma)(bpy)(NO)][PF_6]_2$ (51 mg, 0.057 mmol) and NaN_3 (3.7 mg, 0.057 mmol) in acetone (5 cm^3) was stirred at room temperature for 2 h. A solution of PPh_3 (594 mg, 2.27 mmol) in 2-butanone (10 cm^3) was added, the acetone was removed in vacuo, and the solution was heated at reflux for a further 2 h. The solvent was reduced to a small volume in vacuo and diethyl ether was added to give a golden-coloured precipitate which was filtered off, washed with diethyl ether, and dried. The product was purified by reprecipitation from acetonitrile/diethyl ether to afford a yellow solid. Yield: 45 mg, 80%. *Anal*. Found: C, 46.35; H, 3.80; N, 3.20; P, 6.05. Calc. for $C_{38}H_{39}As_2ClF_6N_2P_2Ru$: C, 46.3; H, 4.00; N, 2.85; P, 6.30%. ^{1}H NMR (200 MHz, CD_3CN): δ 8.34 (2H, d, J = 8.2 Hz, $H^{6,6'}$), 8.24 (2H, d, J = 5.2 Hz, $H^{3,3'}$), 8.07–7.98 (4H, m, $H^{4,4'}$ and C_6H_2), 7.77 (2H, m, C_6H_2), 7.32–7.23 (5H, m, $H^{5,5'}$ and $3PhH^4$), 7.13–7.04 (6H, m, $3PhH^{3,5}$), 6.93 (6H, m, $3PhH^{2,6}$), 1.74 (6H, s, 2AsMe), 1.54 (6H, s, 2AsMe). *m/z*: 841 ($[M-PF_6^-]^+$) and 578 ($[M-PF_6^- - PPh_3]^+$). A reaction was also carried out using the above method, but instead of heating at reflux after the addition of PPh_3, the solution was stirred at room temperature for 93 h. This afforded 26 mg of **2** (46%, pure by ^{1}H NMR).

2.3.3. *trans*-[RuCl(pdma)(bpy)mim]PF_6 (3)

A solution of *trans*-$[RuCl(pdma)(bpy)(NO)][PF_6]_2$ (50 mg, 0.056 mmol) and NaN_3 (3.7 mg, 0.057 mmol) in acetone (5 cm^3) was stirred at room temperature for 2 h. *N*-Methylimidazole (mim, 5 cm^3) was added, the acetone was removed in vacuo, and the solution was heated at ca. 100°C for 1 h. After cooling to room temperature, addition of aqueous NH_4PF_6 and water afforded a red precipitate which was filtered off, washed with water and dried. Reprecipitation from acetone/diethyl ether gave a deep red solid. Yield: 42 mg, 94%. *Anal*. Found: C, 36.2; H, 3.75; N, 7.05. Calc. for

$C_{24}H_{30}As_2ClF_6N_4PRu$: C, 35.75; H, 3.75; N, 6.95%. ^{1}H NMR (200 MHz, CD_3COCD_3): δ 9.53 (2H, d, J = 5.2 Hz, $H^{6,6'}$), 8.72 (2H, d, J = 8.0 Hz, $H^{3,3'}$), 8.21 (2H, t, $H^{4,4'}$), 8.12 (2H, m, C_6H_2), 7.76 (2H, t, $H^{5,5'}$), 7.67 (2H, m, C_6H_2), 7.31 (1H, s, $C_3H_3N_2$), 6.95 (1H, s, $C_3H_3N_2$), 6.36 (1H, s, $C_3H_3N_2$), 3.54 (3H, s, Me), 1.83 (6H, s, 2AsMe), 1.72 (6H, s, 2AsMe). *m/z*: 660 ($[M-PF_6^-]^+$) and 577 ($[M-PF_6^- - mim]^+$).

2.3.4. trans-[RuCl(pdma)(bpy)(MeCN)]PF_6 (4)

This was prepared in a similar manner to **1** by using acetonitrile in place of pyridine. The reaction was cooled to room temperature, and the solvent removed in vacuo. The resulting yellow/orange oil was dissolved in acetone (3 cm^3), and addition of aqueous NH_4PF_6 afforded an orange precipitate which was filtered off, washed with water and dried. Reprecipitation from acetone/diethyl ether yielded an orange solid. Yield: 36 mg, 82%. *Anal*. Found: C, 35.8; H, 4.00; N, 5.00. Calc. for $C_{22}H_{27}As_2ClF_6N_3PRu \cdot 0.5C_3H_6O$: C, 35.55; H, 3.80; N, 5.30%. ^{1}H NMR (200 MHz, CD_3COCD_3): δ 9.50 (2H, d, J = 5.9 Hz, $H^{6,6'}$), 8.73 (2H, d, J = 7.4 Hz, $H^{3,3'}$), 8.27 (2H, t, $H^{4,4'}$), 8.14 (2H, m, C_6H_2), 7.83 (2H, t, $H^{5,5'}$), 7.69 (2H, m, C_6H_2), 2.28 (3H, s, Me), 1.67 (12H, s, 4AsMe). ν(C≡N) 2267 w cm^{-1}. *m/z*: 620 ($[M-PF_6^-]^+$) and 578 ($[M-PF_6^- - MeCN]^+$).

2.3.5. trans-[RuCl(pdma)(bpy)dmso]PF_6 (5)

This was prepared and purified in an identical manner to **3**, but using dmso in place of mim, to afford a yellow solid. Yield: 33 mg, 74%. *Anal*. Found: C, 32.7; H, 3.90; N, 3.40; S, 3.40. Calc. for $C_{22}H_{30}As_2ClF_6N_2OPRuS$: C, 32.95; H, 3.75; N, 3.50; S, 4.00%. ^{1}H NMR (200 MHz, CD_3COCD_3): δ 9.55 (2H, d, J = 4.8 Hz, $H^{6,6'}$), 8.72 (2H, d, J = 7.4 Hz, $H^{3,3'}$), 8.34 (2H, t, $H^{4,4'}$), 8.09 (2H, m, C_6H_2), 7.90 (2H, t, $H^{5,5'}$), 7.69 (2H, m, C_6H_2), 2.96 (6H, s, 2Me), 1.93 (12H, s, 4AsMe). ν(S=O) 1085 m cm^{-1}. *m/z*: 657 ($[M-PF_6^-]^+$) and 579 ($[M-PF_6^- - dmso]^+$).

2.3.6. trans-[RuCl(pdma)(bpy)pyz]PF_6 (6)

This was prepared in an identical manner to **2**, but using pyrazine (181 mg, 2.26 mmol) in place of PPh_3. Reprecipitation from acetone/diethyl ether afforded a red solid. Yield: 37 mg, 78%. *Anal*. Found: C, 36.7; H, 3.50; N, 7.05. Calc. for $C_{24}H_{28}As_2ClF_6N_4PRu \cdot 0.5C_3H_6O$: C, 36.75; H, 3.75; N, 6.75%. ^{1}H NMR (200 MHz, CD_3CN): δ 9.18 (2H, d, J = 5.6 Hz, $H^{6,6'}$), 8.57 (2H, d, J = 8.0 Hz, $H^{3,3'}$), 8.20 (2H, t, $H^{4,4'}$), 8.05 (2H, m, C_6H_2), 7.99 (2H, d, J = 4.6 Hz, pyz), 7.86 (2H, d, J = 4.6 Hz, pyz), 7.73–7.66 (4H, m, $H^{5,5'}$ and C_6H_2), 1.77 (6H, s, 2AsMe), 1.66 (6H, s, 2AsMe). *m/z*: 659 ($[M-PF_6^-]^+$) and 579 ($[M-PF_6^- - pyz]^+$).

2.3.7. trans-[RuCl(pdma)(bpy)($mpyz^+$)][PF_6]$_2$ (7)

A solution of **6** (50 mg, 0.062 mmol) in DMF (1.5 cm^3) and MeI (0.5 cm^3) was stirred at room temperature for 24 h. The excess MeI was removed in vacuo, and addition of aqueous NH_4PF_6 afforded a purple precipitate which was filtered off and washed with water. The crude product was dissolved in acetone and the solution was filtered to remove an insoluble tan residue. Addition of diethyl ether to the filtrate gave a purple precipitate which was filtered off and washed with diethyl ether. Repeated recrystallization from acetonitrile/diethyl ether yielded the purple product. Yield: 11 mg, 18%. *Anal*. Found: C, 32.0; H, 3.55; N, 5.95. Calc. for $C_{25}H_{31}As_2ClF_{12}N_4P_2Ru \cdot 0.5C_2H_3N$: C, 31.7; H, 3.35; N, 6.40%. ^{1}H NMR (200 MHz, CD_3COCD_3): δ 9.22 (2H, d, J = 4.8 Hz, $H^{6,6'}$), 8.99 (2H, d, J = 5.3 Hz, $mpyz^+$), 8.89 (2H, d, J = 8.2 Hz, $H^{3,3'}$), 8.40 (2H, t, $H^{4,4'}$), 8.21 (4H, m, C_6H_2 and $mpyz^+$), 7.85 (2H, t, $H^{5,5'}$), 7.77 (2H, m, C_6H_2), 3.98 (3H, s, Me), 1.90 (6H, s, 2AsMe), 1.88 (6H, s, 2AsMe). *m/z*: 819 ($[M-PF_6^-]^+$) and 579 ($[M-2PF_6^- - mpyz]^+$).

2.3.8. trans-[RuCl(pdma)(phen)py]PF_6 (8)

This was prepared and purified in an identical manner to **1** by using *trans*-[RuCl(pdma)(phen)(NO)][PF_6]$_2$ (100 mg, 0.108 mmol) in place of *trans*-[RuCl(pdma)(bpy)(NO)][PF_6]$_2$. A red solid was obtained. Yield: 80 mg, 89%. *Anal*. Found: C, 39.3; H, 3.70; N, 5.05. Calc. for $C_{27}H_{29}As_2ClF_6N_3PRu$: C, 39.2; H, 3.55; N, 5.10%. ^{1}H NMR (200 MHz, CD_3CN): δ 9.66 (2H, d, J = 5.2 Hz, $H^{2,9}$), 8.72 (2H, d, J = 8.2 Hz, $H^{4,7}$), 8.24 (2H, s, $H^{5,6}$), 8.11–8.01 (4H, m, $H^{3,8}$ and C_6H_2), 7.86 (2H, d, J = 6.4 Hz, $pyH^{2,6}$), 7.72 (2H, m, C_6H_2), 7.49 (1H, t, pyH^4), 6.84 (2H, t, $pyH^{3,5}$), 1.87 (6H, s, 2AsMe), 1.69 (6H, s, 2AsMe). *m/z*: 682 ($[M-PF_6^-]^+$) and 603 ($[M-PF_6^- - py]^+$).

2.3.9. trans-[RuCl(pdma)(phen)PPh_3]PF_6 (9)

This was prepared and purified in an identical manner to **2** by using *trans*-[RuCl(pdma)(phen)(NO)][PF_6]$_2$ (100 mg, 0.108 mmol) in place of *trans*-[RuCl(pdma)(bpy)(NO)][PF_6]$_2$. A yellow solid was obtained. Yield: 88 mg, 80%. *Anal*. Found: C, 47.2; H, 3.95; N, 3.00; P, 6.00. Calc. for $C_{40}H_{39}As_2ClF_6N_2P_2Ru$: C, 47.55; H, 3.90; N, 2.75; P, 6.15%. ^{1}H NMR (200 MHz, CD_3COCD_3): δ 9.09 (2H, d, J = 4.6 Hz, $H^{2,9}$), 8.75 (2H, d, J = 7.2 Hz, $H^{4,7}$), 8.27 (2H, s, $H^{5,6}$), 8.23 (2H, m, C_6H_2), 7.82 (4H, m, $H^{3,8}$ and C_6H_2), 7.31 (3H, t, $3PhH^4$), 7.08 (6H, t, $3PhH^{3,5}$), 6.75 (6H, t, $3PhH^{2,6}$), 1.94 (6H, s, 2AsMe), 1.70 (6H, s, 2AsMe). *m/z*: 864 ($[M-PF_6^-]^+$) and 602 ($[M-PF_6^- - PPh_3]^+$).

2.3.10. trans-[RuCl(pdma)(phen)mim]PF_6 (10)

This was prepared and purified in an identical manner to **3** by using *trans*-[RuCl(pdma)(phen)(NO)][PF_6]$_2$ (200 mg, 0.217 mmol) in place of *trans*-[RuCl(pdma)(bpy)(NO)][PF_6]$_2$. A red solid was obtained. Yield: 158 mg, 82%. *Anal*. Found: C, 38.85; H, 4.20; N, 6.35. Calc. for $C_{26}H_{30}As_2ClF_6N_4PRu \cdot C_3H_6O$: C, 39.25; H, 4.10; N, 6.30%. ^{1}H NMR (200 MHz, CD_3COCD_3): δ 9.94 (2H, d, J = 5.0 Hz, $H^{2,9}$), 8.81 (2H, d, J = 8.2 Hz, $H^{4,7}$), 8.32 (2H, s, $H^{5,6}$), 8.14 (4H, m, $H^{3,8}$ and C_6H_2), 7.70 (2H, m, C_6H_2), 7.22 (1H, s, $C_3H_3N_2$), 6.85 (1H, s, $C_3H_3N_2$), 6.33 (1H, s, $C_3H_3N_2$), 3.42 (3H, s, Me), 1.92 (6H, s, 2AsMe), 1.81 (6H, s,

2AsMe). *m/z*: 684 ([M−PF_6^-]$^+$) and 603 ([M−PF_6^-−mim]$^+$).

*2.3.11. trans-[RuCl(pdma)(phen)pyz]PF_6 (**11**)*

This was prepared and purified in an identical manner to **6** by using *trans*-[RuCl(pdma)(phen)(NO)][PF_6]$_2$ (100 mg, 0.108 mmol) in place of *trans*-[RuCl(pdma)-(bpy)(NO)][PF_6]$_2$. A red solid was obtained. Yield: 80 mg, 89%. *Anal*. Found: C, 37.75; H, 3.60; N, 6.50. Calc. for $C_{26}H_{28}As_2ClF_6N_4PRu$: C, 37.7; H, 3.40; N, 6.75%. ^{1}H NMR (200 MHz, CD_3CN): δ 9.68 (2H, d, J=4.4 Hz, $H^{2,9}$), 8.76 (2H, d, J=6.0 Hz, $H^{4,7}$), 8.26 (2H, s, $H^{5,6}$), 8.13–8.02 (4H, m, $H^{3,8}$ and C_6H_2), 7.89 (4H, m, pyz), 7.73 (2H, m, C_6H_2), 1.86 (6H, s, 2AsMe), 1.73 (6H, s, 2AsMe). *m/z*: 683 ([M−PF_6^-]$^+$) and 603 ([M−PF_6^-−pyz]$^+$).

*2.3.12. trans-[RuCl(pdma)(phen)(mpyz$^+$)][PF_6]$_2$ (**12**)*

This was prepared and purified in an identical manner to **7**, but using **11** (50 mg, 0.061 mmol) in place of **6**. A deep purple solid was obtained. Yield: 29 mg, 48%. *Anal*. Found: C, 32.8; H, 3.05; N, 5.50. Calc. for $C_{27}H_{31}As_2ClF_{12}N_4P_2Ru$: C, 32.85; H, 3.15; N, 5.65%. ^{1}H NMR (200 MHz, CD_3COCD_3): δ 9.66 (2H, d, J=5.2 Hz, $H^{2,9}$), 8.99 (4H, m, $H^{4,7}$ and mpyz$^+$), 8.44 (2H, s, $H^{5,6}$), 8.27–8.12 (6H, m, $H^{3,8}$, C_6H_2 and mpyz$^+$), 7.79 (2H, m, C_6H_2) 3.93 (3H, s, Me), 1.99 (6H, s, 2AsMe), 1.97 (6H, s, 2AsMe). *m/z*: 843 ([M−PF_6^-]$^+$), 698 ([M−2PF_6^-]$^+$) and 602 ([M−2PF_6^-−mpyz$^+$]$^+$).

*2.3.13. trans-[Ru(pdma)(bpy)(mim)$_2$][PF_6]$_2$ (**13**)*

A solution of **3** (50 mg, 0.062 mmol), $AgCF_3CO_2$ (13.8 mg, 0.062 mmol) and mim (0.2 cm^3) in acetone (5 cm^3) was heated at reflux for 75 min. Water (5 cm^3) was added, and reflux was continued for a further 3 h. The reaction mixture was then filtered through celite to remove AgCl, and addition of aqueous NH_4PF_6 and water yielded an orange precipitate, which was filtered off, washed with water, and dried. Reprecipitation from acetone/diethyl ether afforded an orange solid. Yield: 50 mg, 81%. *Anal*. Found: C, 34.0; H, 3.45; N, 8.50. Calc. for $C_{28}H_{36}As_2F_{12}N_6P_2Ru$: C, 33.7; H, 3.65; N, 8.45%. ^{1}H NMR (200 MHz, CD_3COCD_3): δ 9.61 (2H, d, J=4.8 Hz, $H^{6,6'}$), 8.78 (2H, d, J=8.0 Hz, $H^{3,3'}$), 8.36 (2H, t, $H^{4,4'}$), 8.25 (2H, m, C_6H_2), 7.91 (2H, t, $H^{5,5'}$), 7.78 (2H, m, C_6H_2), 7.22 (2H, s, 2$C_3H_3N_2$), 6.96 (2H, s, 2$C_3H_3N_2$), 6.25 (2H, s, 2$C_3H_3N_2$), 3.49 (6H, s, 2Me), 1.80 (12H, s, 4AsMe). *m/z*: 852 ([M−PF_6^-]$^+$), 707 ([M−2PF_6^-]$^+$), 624 ([M−2PF_6^-–mim]$^+$) and 543 ([M−2PF_6^-−2mim]$^+$).

*2.3.14. trans-[Ru(pdma)(bpy)(mim)py][PF_6]$_2$ (**14**)*

This was prepared and purified in an identical fashion to **13** but using pyridine (0.4 cm^3) in place of mim. A yellow/orange solid was obtained. Yield: 43 mg, 66%. *Anal*. Found: C, 36.5; H, 3.65; N, 6.65. Calc. for $C_{29}H_{35}As_2F_{12}N_5P_2Ru\cdot C_3H_6O$: C, 36.5; H, 3.95; N, 6.65%. ^{1}H NMR (200 MHz, CD_3COCD_3): δ 9.69 (2H, d, J=4.6 Hz, $H^{6,6'}$), 8.76 (2H, d, J=8.0 Hz, $H^{3,3'}$), 8.35 (2H, t, $H^{4,4'}$), 8.29–8.24 (4H, m, $pyH^{2,6}$ and C_6H_2), 7.96 (2H, t, $H^{5,5'}$), 7.82–7.76 (3H, m, pyH^4 and C_6H_2), 7.22–7.12 (3H, m, $pyH^{3,5}$ and $C_3H_3N_2$), 6.97 (1H, s, $C_3H_3N_2$), 6.15 (1H, s, $C_3H_3N_2$), 3.47 (3H, s, Me), 1.91 (6H, s, 2AsMe), 1.80 (6H, s, 2AsMe). *m/z*: 849 ([M−PF_6^-]$^+$), 703 ([M−2PF_6^-]$^+$), 624 ([M−2PF_6^-−py]$^+$) and 543 ([M−2PF_6^-−py–mim]$^+$).

*2.3.15. trans-[Ru(pdma)(bpy)(mim)MeCN][PF_6]$_2$ (**15**)*

This was prepared in an identical fashion to **13** but using acetonitrile (0.4 cm^3) in place of mim, with no reprecipitation of the crude product. An orange solid was obtained. Yield: 52 mg, 88%. *Anal*. Found: C, 32.7; H, 3.50; N, 7.70. Calc. for $C_{26}H_{33}As_2F_{12}N_5P_2Ru$: C, 32.65; H, 3.50; N, 7.30%. ^{1}H NMR (200 MHz, CD_3COCD_3): δ 9.46 (2H, d, J=5.4 Hz, $H^{6,6'}$), 8.87 (2H, d, J=8.0 Hz, $H^{3,3'}$), 8.45 (2H, t, $H^{4,4'}$), 8.26 (2H, m, C_6H_2), 7.93 (2H, t, $H^{5,5'}$), 7.79 (2H, m, C_6H_2), 7.20 (1H, s, $C_3H_3N_2$), 7.01 (1H, s, $C_3H_3N_2$), 6.20 (1H, s, $C_3H_3N_2$), 3.50 (3H, s, $C_3H_3N_2$–*Me*), 2.24 (3H, s, Me), 1.94 (6H, s, 2AsMe), 1.90 (6H, s, 2AsMe). *m/z*: 811 ([M−PF_6^-]$^+$), 666 ([M−2PF_6^-]$^+$), 625 ([M−2PF_6^-−MeCN]$^+$) and 544 ([M−2PF_6^-−MeCN−mim]$^+$).

*2.3.16. trans-[Ru(pdma)(bpy)(PPh_3)(MeCN)][PF_6]$_2$ (**16**)*

This was prepared and purified in an identical manner to **15** by using **2** (50 mg, 0.051 mmol) in place of **3**. A yellow solid was obtained. Yield: 37 mg, 64%. *Anal*. Found: C, 41.95; H, 3.75; N, 3.70; P, 7.85. Calc. for $C_{40}H_{42}As_2F_{12}N_3P_3Ru$: C, 42.25; H, 3.70; N, 3.70; P, 8.20%. ^{1}H NMR (200 MHz, CD_3COCD_3): δ 8.92 (2H, d, J=5.0 Hz, $H^{6,6'}$), 8.65 (2H, d, J=7.6 Hz, $H^{3,3'}$), 8.30 (4H, m, $H^{4,4'}$ and C_6H_2), 7.89 (2H, m, C_6H_2), 7.74 (2H, t, $H^{5,5'}$), 7.40 (3H, t, $3PhH^4$), 7.15 (6H, t, $3PhH^{3,5}$), 6.76 (6H, t, $3PhH^{2,6}$), 2.22 (3H, s, Me), 1.96 (6H, s, 2AsMe), 1.66 (6H, s, 2AsMe). *m/z*: 991 ([M−PF_6^-]$^+$), 845 ([M−2PF_6^-]$^+$), 583 ([M−2PF_6^-−PPh_3]$^+$) and 542 ([M−2PF_6^-−PPh_3−MeCN]$^+$).

*2.3.17. cis-[RuCl(pdma)(bpy)mim]PF_6 (**17**)*

A solution of **3** (40 mg, 0.050 mmol) in acetone (20 cm^3) was exposed to sunlight for 100 h, during which time the isomerization was completed (as shown by ^{1}H NMR spectroscopy on a smaller sample in acetone-d_6). The addition of diethyl ether gave a precipitate which was filtered off, washed with diethyl ether and dried to afford a deep red solid. Yield: 31 mg, 78%. *Anal*. Found: C, 35.9; H, 4.00; N, 7.05. Calc. for $C_{24}H_{30}As_2ClF_6N_4PRu$: C, 35.75; H, 3.75; N, 6.95%. ^{1}H NMR (200 MHz, CD_3COCD_3): δ 9.96 (1H, d, J=6.0 Hz, bpy), 8.97 (1H, d, J=5.4 Hz, bpy), 8.56 (2H, t, bpy), 8.12 (1H, t, bpy), 8.10–7.99 (2H, m, C_6H_2), 7.93–7.80 (3H, m, bpy and $C_3H_3N_2$), 7.65–7.58 (2H, m, C_6H_2), 7.46 (1H, t, bpy), 7.09 (1H, s, $C_3H_3N_2$), 6.74 (1H, s, $C_3H_3N_2$), 3.71 (3H, s, $C_3H_3N_2$–*Me*), 1.92 (3H, s, AsMe), 1.56 (3H, s, AsMe), 1.48 (3H, s, AsMe), 0.74 (3H, s, AsMe). *m/z*: 661 ([M−PF_6^-]$^+$) and 579 ([M−PF_6^-−mim]$^+$).

2.4. X-ray crystallography

Crystals of **1**, **3**, **12**·3MeCN and **17** were grown by slow diffusion of diethyl ether vapour into acetonitrile solutions of the complex salts at 4°C. Those of **2**·DMF and **14**·DMF were obtained in similar manner, but using DMF solutions. The approximate dimensions (mm) of the crystals chosen for diffraction studies were as follows: **1** (0.15×0.15×0.10), **2**·DMF (0.40×0.10×0.10), **3** (0.40×0.20×0.05), **12**·3MeCN (0.15×0.15×0.05), **14**·DMF (0.30×0.20×0.05), **17** (0.10×0.10×0.05).

Data collection details are as follows: for **1**, **2**·DMF and **3** data were collected on a Siemens SMART CCD area-detector diffractometer. Empirical absorption corrections were applied by using multiple measurements of equivalent reflections, and the data were integrated by using SAINT [13]. For **12**·3MeCN, **14**·DMF and **17** data were collected on a Nonius Kappa CCD area-detector diffractometer controlled by the Collect software package [14]. The data were processed by Denzo [15] and corrected for absorption by using the empirical method employed in Sortav [16,17] from within the MAXUS suite of programs [18].

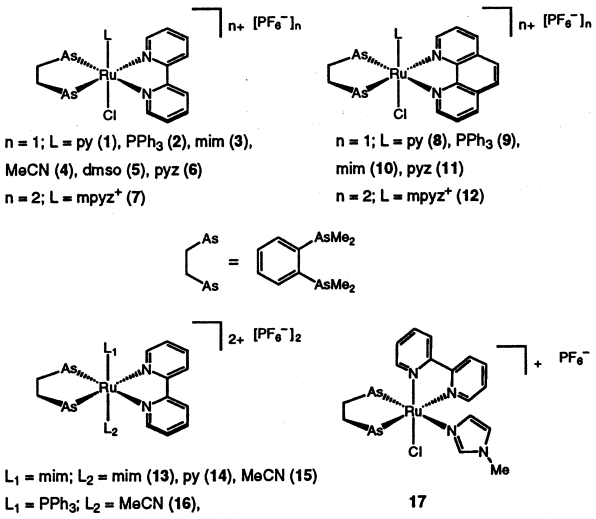

The structures of **1**, **2**·DMF and **3** were solved by direct methods and refined by full-matrix least-squares on all F_o^2 data using Siemens SHELXTL 5.03 [13]. The same approach was used for **12**·3MeCN, **14**·DMF and **17**, but using SHELXS-90 [19] and SHELXL-97 [20]. In all cases, all non-hydrogen atoms were refined anisotropically with hydrogen atoms included in idealized positions with thermal parameters riding on those of the parent atom. Static disorder is present in the PF_6^- anions of **1** and **17**, and in the axial ligands of **14**·DMF (50% occupancy by py and mim in both positions).

Representations of the complex cations in **1**, **2**·DMF, **3**, **12**·3MeCN, **14**·DMF and **17** are given in Figs. 1–6. Crystallographic data and refinement details are presented in Table 1, and selected bond distances and angles in Table 2.

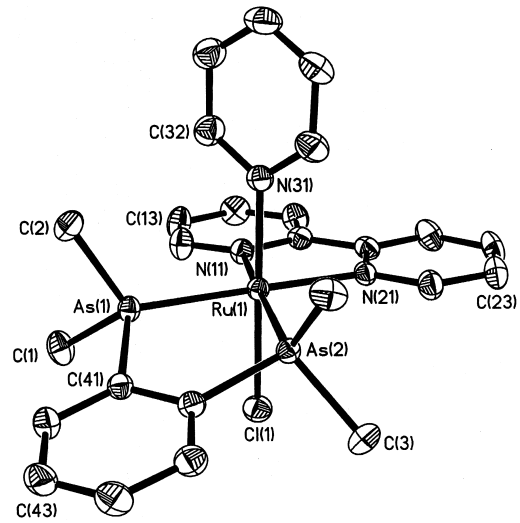

Fig. 1. Structural representation of the complex cation in the salt **1**, with hydrogen atoms omitted (50% probability ellipsoids).

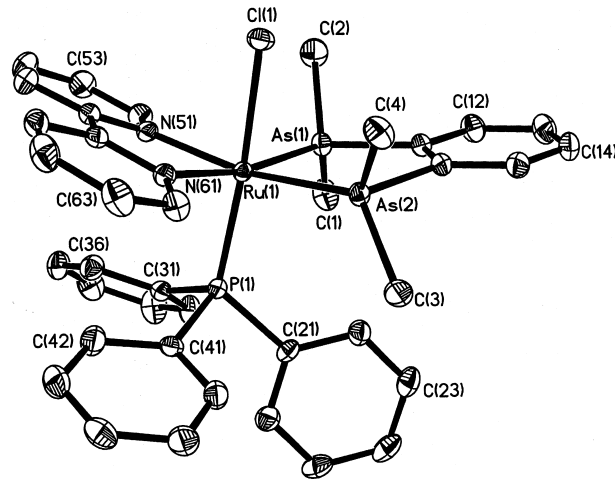

Fig. 2. Structural representation of the complex cation in the salt **2**·DMF, with hydrogen atoms omitted (50% probability ellipsoids).

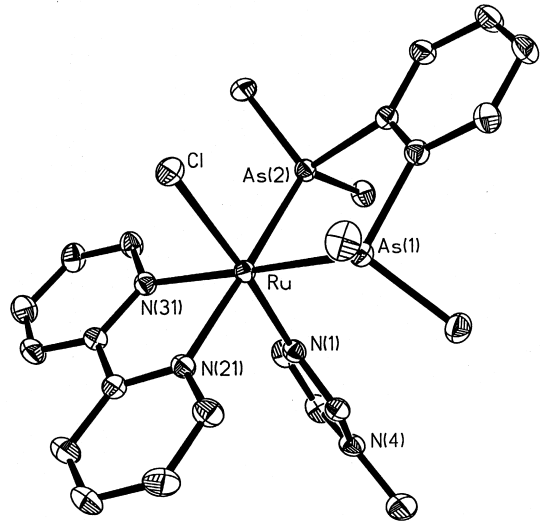

Fig. 3. Structural representation of the complex cation in the salt **3**, with hydrogen atoms omitted (50% probability ellipsoids).

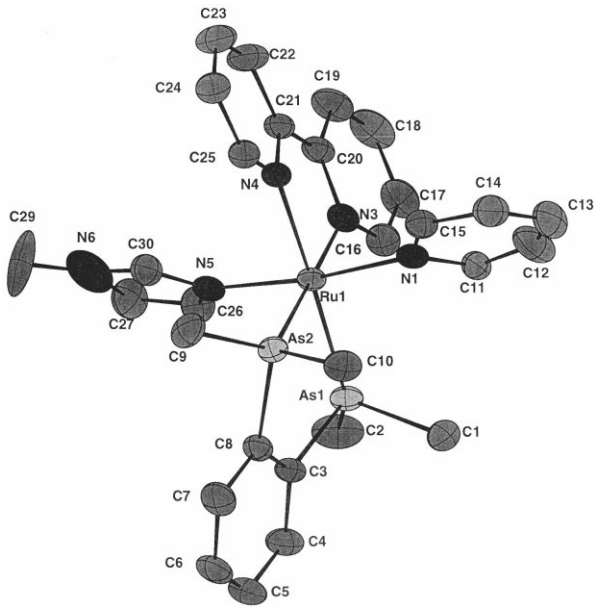

Fig. 4. Structural representation of the complex cation in the salt **12**·3MeCN, with disorder removed and hydrogen atoms omitted (50% probability ellipsoids).

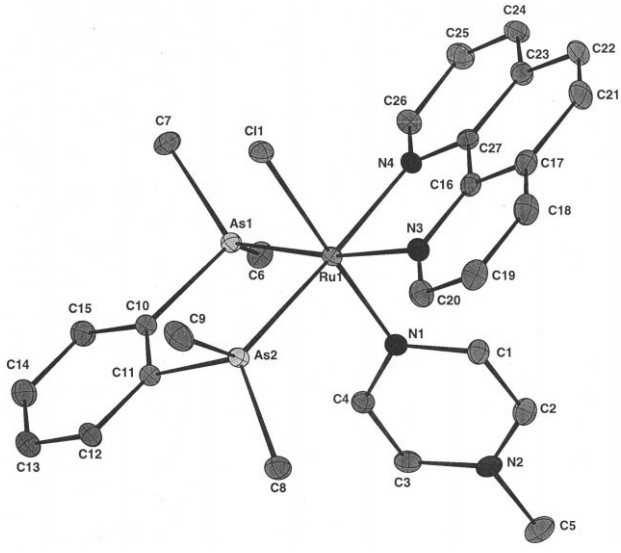

Fig. 5. Structural representation of the complex cation in the salt **14**·DMF, with hydrogen atoms omitted (50% probability ellipsoids).

3. Results and discussion

3.1. Synthesis and characterization

It is well established that sufficiently electrophilic, linearly coordinated nitrosyl ligands react with nucleophiles [21,22], and the reaction with azide ion is a versatile means to convert ruthenium(II) nitrosyls into substituted derivatives via dinitrogen or solvento intermediates [10,11,23–25]. The ν(NO) values in *trans*-[$Ru^{II}Cl(pdma)(L–L)(NO)][PF_6]_2$, 1878 cm^{-1} (L–L = bpy) and 1874 cm^{-1} (L–L = phen) [12], are indicative of relatively electron-deficient nitrosyl ligands [21,22], and these complexes hence react readily with stoi-

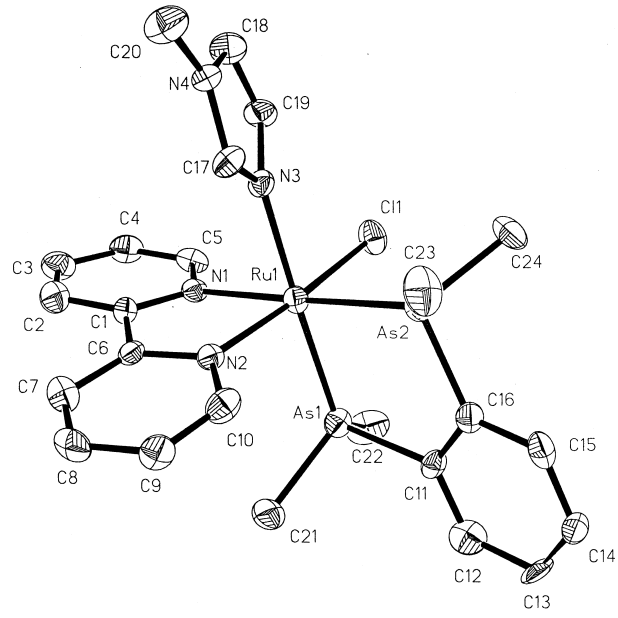

Fig. 6. Structural representation of the complex cation in the salt **17**, with hydrogen atoms omitted (50% probability ellipsoids).

chiometric azide at room temperature in acetone. The resulting intermediates, most likely *trans*-[$Ru^{II}Cl(pdma)(L–L)N_2]^+$, react with a range of neutral ligands to give clean substitution of the position formerly occupied by NO^+. These reactions take place only slowly at room temperature, but occur much more rapidly upon heating at ca. 80°C in 2-butanone.

Unlike the related complexes *trans*-[$Ru^{II}Cl(pdma)_2L]^+$ (L = py, mim, etc.) [10], the pdma/L–L *trans* mixed-chelates react with neutral ligands in the presence of $AgCF_3CO_2$ to substitute the chloride ligands, although heating is required to give reasonably efficient reactions. For example, **15** was also isolated from a reaction at room temperature, but in a yield of only 14%. The efficacy of these substitution reactions depends to varying degrees upon the nature of the starting complex and the incoming ligand. The best results were obtained with salt **3**, from which the derivatives **13**–**15** were prepared. The presence of the *trans* geometry in the salts **1**–**16** is confirmed by the ^{1}H NMR spectra which each show a single AA′BB′ pattern for the pdma ligand, either one or two singlets for the AsMe groups and four signals for bpy or phen.

3.2. Photoisomerization reactions

Previous studies have shown that *trans*-{$Ru^{II}(L–L)_2\}^{2+}$ (L–L = bpy or phen) complexes readily photoisomerize to their more stable *cis* isomers [8,26]. By contrast, when L–L = pdma, no evidence for photoinstability has been found [10]. Given these observations, it is perhaps unsurprising that the new *trans*-{Ru(pdma)(L–L)$\}^{2+}$ (L–L = bpy or phen) complexes show an intermediate degree of photostability. ^{1}H NMR experiments in d_6-acetone show that salts **1**–**16** undergo complete isomerization to their *cis* forms, with partial decomposition in some cases, following exposure to

Table 1
Crystallographic data and refinement details for the complex salts **1**, **2**·DMF, **3**, **12**·3MeCN, **14**·DMF and **17**

	1	**2**·DMF	**3**	**12**·3MeCN	**14**·DMF	**17**
Formula	$C_{25}H_{29}As_2ClF_6N_3PRu$	$C_{41}H_{46}As_2ClF_6N_3OP_2Ru$	$C_{24}H_{30}As_2ClF_6N_4PRu$	$C_{33}H_{40}As_2ClF_{12}N_7P_2Ru$	$C_{32}H_{42}As_2F_{12}N_6OP_2Ru$	$C_{24}H_{30}As_2ClF_6N_4PRu$
FW	802.84	1059.11	805.85	1111.02	1067.57	805.85
Crystal system	monoclinic	monoclinic	monoclinic	triclinic	triclinic	orthorhombic
Space group	$P2_1/c$	$P2_1/n$	$P2_1/c$	$P\bar{1}$	$P\bar{1}$	$Pbca$
a (Å)	10.4102(12)	14.686(2)	10.560(3)	11.707(2)	11.837(2)	8.9694(4)
b (Å)	15.609(3)	10.4026(9)	15.673(2)	12.217(2)	13.049(3)	16.5043(9)
c (Å)	17.438(2)	28.806(4)	17.413(4)	16.562(3)	15.315(3)	39.139(2)
α (°)				72.40(3)	83.81(3)	
β (°)	95.828(9)	103.878(7)	96.25(2)	80.24(3)	71.56(3)	
γ (°)				73.40(3)	67.15(3)	
U (Å^3)	2818.8(6)	4272.1(8)	2865.0(10)	2154.8(6)	2067.7(7)	5793.9(5)
Z	4	4	4	2	2	8
D_c (Mg m^{-3})	1.892	1.647	1.868	1.712	1.718	1.848
Temperature (K)	173(2)	173(2)	173(2)	150(2)	293(2)	150(2)
λ (Å)	0.710 73 (Mo Kα)	0.710 73 (Mo Kα)	0.710 73 (Mo Kα)	0.710 73 (Mo Kα)	0.710 73 (Mo Kα)	0.710 73 (Mo Kα)
$F(000)$	1584	2128	1592	1104	1066	3184
μ (mm^{-1})	3.099	2.105	3.051	2.110	2.135	3.017
Scan type	$\varphi+\omega$	$\varphi+\omega$	$\varphi+\omega$	$\varphi+\omega$	$\varphi+\omega$	$\varphi+\omega$
θ Range (°)	1.76–27.49	1.46–27.47	1.75–27.49	1.82–26.39	1.69–26.00	2.47–25.25
h, k, l ranges	±13, ±20, ±22	±19, ±13, ±37	−13/11, −20/16, ±22	±14, ±15, ±20	±14, ±16, ±19	±10, ±19, −40/46
Reflections collected	28629	42781	18047	44788	44404	35774
Unique reflections (R_{int})	6469 (0.0415)	9784 (0.0351)	6559 (0.0410)	8820 (0.0576)	8109 (0.0453)	5183 (0.1204)
Data/restraints/parameters	6468/221/410	9784/0/520	6559/0/352	8820/0/558	8089/72/532	5183/22/401
Final R indices ($I>2\sigma(I)$) [a,b]	$R_1=0.0298$, $wR_2=0.0629$	$R_1=0.0293$, $wR_2=0.0649$	$R_1=0.0321$, $wR_2=0.0663$	$R_1=0.0307$, $wR_2=0.0995$	$R_1=0.0471$, $wR_2=0.1612$	$R_1=0.0480$, $wR_2=0.0843$
Final R indices (all data)	$R_1=0.0473$, $wR_2=0.0697$	$R_1=0.0418$, $wR_2=0.0687$	$R_1=0.0577$, $wR_2=0.0746$	$R_1=0.0357$, $wR_2=0.1058$	$R_1=0.0542$, $wR_2=0.1693$	$R_1=0.1019$, $wR_2=0.0937$
Weighting factors (x, y) [b]	0.0335, 0.3513	0.0301, 2.0533	0.0364, 0	0.1000, 0	0.1000, 0	0.0411, 0
Goodness of fit, (S)	1.038	1.092	0.935	0.873	1.379	0.934
Peak and hole (e Å^{-3})	0.666, −0.720	1.118, −0.810	0.551, −0.694	1.067, −0.764	0.986, −0.979	1.126, −0.688

[a] Structures were refined on F_o^2 using all data; the values of R_1 are given for comparison with older refinements based on F_o with a typical threshold of $F_o>4\sigma(F_o)$.
[b] $wR_2=[\sum w(F_o^2-F_c^2)^2/\sum w(F_o^2)^2]^{1/2}$; $S=[\sum w(F_o^2-F_c^2)^2/(M-N)]^{1/2}$ where M is the number of reflections and N is the number of parameters; $w^{-1}=[\sigma^2(F_o^2)+(xP)^2+yP]$ and $P=[\max(F_o^2,0)+2F_c^2]/3$.

Table 2
Selected bond distances (Å) and angles (°) for the complex salts **1**, **2**·DMF, **3**, **12**·3MeCN, **14**·DMF and **17**

1			
Ru(1)–N(31)	2.088(3)	Ru(1)–As(1)	2.4117(6)
Ru(1)–N(21)	2.103(3)	Ru(1)–As(2)	2.4186(5)
Ru(1)–N(11)	2.108(3)	Ru(1)–Cl(1)	2.4254(10)
N(31)–Ru(1)–N(21)	87.36(11)	N(11)–Ru(1)–As(2)	173.18(8)
N(31)–Ru(1)–N(11)	87.90(11)	As(1)–Ru(1)–As(2)	82.123(13)
N(21)–Ru(1)–N(11)	77.88(11)	N(31)–Ru(1)–Cl(1)	175.06(8)
N(31)–Ru(1)–As(1)	93.63(8)	N(21)–Ru(1)–Cl(1)	90.49(8)
N(21)–Ru(1)–As(1)	178.74(8)	N(11)–Ru(1)–Cl(1)	87.30(8)
N(11)–Ru(1)–As(1)	101.38(8)	As(1)–Ru(1)–Cl(1)	88.45(2)
N(31)–Ru(1)–As(2)	97.77(8)	As(2)–Ru(1)–Cl(1)	86.95(3)
N(21)–Ru(1)–As(2)	98.51(7)		
2·DMF			
Ru(1)–N(61)	2.093(2)	Ru(1)–As(1)	2.4160(4)
Ru(1)–N(51)	2.101(2)	Ru(1)–As(2)	2.4278(4)
Ru(1)–P(1)	2.2947(7)	Ru(1)–Cl(1)	2.4629(7)
N(61)–Ru(1)–N(51)	78.23(8)	P(1)–Ru(1)–As(2)	98.55(2)
N(61)–Ru(1)–P(1)	92.26(6)	As(1)–Ru(1)–As(2)	84.727(12)
N(51)–Ru(1)–P(1)	93.60(6)	N(61)–Ru(1)–Cl(1)	84.45(6)
N(61)–Ru(1)–As(1)	168.98(6)	N(51)–Ru(1)–Cl(1)	83.41(6)
N(51)–Ru(1)–As(1)	97.76(6)	P(1)–Ru(1)–Cl(1)	175.93(2)
P(1)–Ru(1)–As(1)	98.27(2)	As(1)–Ru(1)–Cl(1)	84.90(2)
N(61)–Ru(1)–As(2)	96.97(6)	As(2)–Ru(1)–Cl(1)	84.24(2)
N(51)–Ru(1)–As(2)	167.13(6)		
3			
Ru–N(1)	2.087(3)	Ru(1)–As(1)	2.4081(7)
Ru–N(21)	2.107(3)	Ru(1)–As(2)	2.4028(5)
Ru–N(31)	2.107(3)	Ru(1)–Cl	2.4494(11)
N(1)–Ru–N(21)	87.36(11)	N(21)–Ru–Cl	90.41(8)
N(1)–Ru–N(31)	87.32(11)	N(31)–Ru–As(1)	174.64(8)
N(1)–Ru–As(1)	96.99(8)	N(31)–Ru–As(2)	100.84(8)
N(1)–Ru–As(2)	93.20(7)	N(31)–Ru–Cl	88.43(8)
N(1)–Ru–Cl	175.55(8)	As(1)–Ru–Cl	87.18(3)
N(21)–Ru–N(31)	77.47(11)	As(1)–Ru–As(2)	82.16(2)
N(21)–Ru–As(1)	99.48(8)	As(2)–Ru–Cl	88.91(3)
N(21)–Ru–As(2)	178.20(8)		
12·3MeCN			
Ru(1)–N(1)	2.019(2)	Ru(1)–As(1)	2.4067(9)
Ru(1)–N(3)	2.120(2)	Ru(1)–As(2)	2.4182(7)
Ru(1)–N(4)	2.118(2)	Ru(1)–Cl(1)	2.4146(10)
N(1)–Ru(1)–N(4)	92.49(8)	N(1)–Ru(1)–N(3)	92.28(8)
N(4)–Ru(1)–N(3)	78.39(9)	N(1)–Ru(1)–As(1)	94.82(6)
N(4)–Ru(1)–As(1)	96.84(6)	N(3)–Ru(1)–As(1)	171.62(6)
N(1)–Ru(1)–Cl(1)	176.24(6)	N(4)–Ru(1)–Cl(1)	87.56(6)
N(3)–Ru(1)–Cl(1)	84.04(6)	As(1)–Ru(1)–Cl(1)	88.90(3)
N(1)–Ru(1)–As(2)	90.59(6)	N(4)–Ru(1)–As(2)	176.81(5)
N(3)–Ru(1)–As(2)	100.64(6)	As(1)–Ru(1)–As(2)	83.74(3)
Cl(1)–Ru(1)–As(2)	89.31(3)		
14·DMF			
Ru(1)–N(3)	2.11(2)	Ru(1)–N(1)	2.10(2)
Ru(1)–N(4)	2.11(2)	Ru(1)–N(5)	2.12(2)
Ru(1)–As(1)	2.439(3)	Ru(1)–As(2)	2.447(3)
N(3)–Ru(1)–N(1)	88.1(8)	N(3)–Ru(1)–N(4)	77.7(8)
N(1)–Ru(1)–N(4)	89.2(8)	N(3)–Ru(1)–N(5)	87.0(8)
N(1)–Ru(1)–N(5)	173.0(7)	N(4)–Ru(1)–N(5)	84.8(8)
N(3)–Ru(1)–As(1)	99.8(6)	N(1)–Ru(1)–As(1)	94.5(5)
N(4)–Ru(1)–As(1)	175.5(5)	N(5)–Ru(1)–As(1)	91.3(6)
N(3)–Ru(1)–As(2)	179.3(6)	N(1)–Ru(1)–As(2)	92.4(5)
N(4)–Ru(1)–As(2)	101.9(6)	N(5)–Ru(1)–As(2)	92.5(5)
As(1)–Ru(1)–As(2)	80.61(9)		
17			
Ru(1)–N(1)	2.101(4)	Ru(1)–N(2)	2.056(4)
Ru(1)–N(3)	2.122(4)	Ru(1)–As(1)	2.3686(7)
Ru(1)–As(2)	2.3836(7)	Ru(1)–Cl(1)	2.4377(14)
N(1)–Ru(1)–N(2)	78.46(18)	N(1)–Ru(1)–N(3)	85.04(16)
N(2)–Ru(1)–N(3)	89.36(16)	N(1)–Ru(1)–As(1)	97.58(11)
N(2)–Ru(1)–As(1)	91.04(12)	N(3)–Ru(1)–As(1)	177.37(12)
N(1)–Ru(1)–As(2)	177.06(12)	N(2)–Ru(1)–As(2)	100.13(12)
N(3)–Ru(1)–As(2)	92.38(12)	As(1)–Ru(1)–As(2)	85.00(2)
N(1)–Ru(1)–Cl(1)	92.83(13)	N(2)–Ru(1)–Cl(1)	171.26(13)
N(3)–Ru(1)–Cl(1)	90.69(12)	As(1)–Ru(1)–Cl(1)	89.31(4)
As(2)–Ru(1)–Cl(1)	88.60(4)		

diffuse sunlight for ca. 100 h. The isomerized samples show no reversion to their *trans* forms after extended periods in the dark. The ^{1}H NMR spectra of the *cis* isomers are characterized by increased numbers of signals due to reduced symmetry, together with shifts of as much as 1 ppm for some of the resonances. In particular, the lowest field bpy/phen doublets are shifted downfield and some of the AsMe signals shift upfield, upon *trans* → *cis* isomerization. In the case of the two forms of $[Ru^{II}Cl(pdma)(bpy)mim]PF_6$ (**3** and **17**), the isomerization was further confirmed by X-ray structural studies (see later).

3.3. UV–visible studies

Electronic absorption spectra for all of the new complex salts were recorded in acetonitrile and results are presented in Table 3. All show relatively intense, broad $d_\pi(Ru^{II}) \rightarrow \pi^*$(bpy/phen) MLCT bands [27,28] in the region 360–460 nm. For the series *trans*-$[Ru^{II}Cl(pdma)(bpy)L_1][PF_6]_n$ ($n = 1$ or 2, **1**–**5** and **7**), the MLCT energy decreases as the overall electron donor strength of L_1 increases, in the order L_1 = dmso < $PPh_3 \approx mpyz^+$ < MeCN < py < mim. This ordering reflects a steady destabilization of the Ru-based HOMO. Similar trends are observed for the phen complexes in **8**–**10** and **12** and for the *trans*-$[Ru(pdma)(bpy)mim(L_2)][PF_6]_2$ series **13**–**15**. The disubstituted derivatives **13**–**15** all have higher MLCT energies than their parent complex in **3** because mim, py and MeCN are less basic than chloride. For the same reasons, substitution of the chloride ligand in **2** by MeCN to give **16** produces a blue shift of ca. 0.25 eV.

The complexes containing py or pyz co-ligands also show $d_\pi(Ru^{II}) \rightarrow \pi^*$(py/pyz) MLCT bands which in many cases overlap with the $d_\pi(Ru^{II}) \rightarrow \pi^*$(bpy/phen) absorptions. In the complexes in **7** and **12**, $d_\pi(Ru^{II}) \rightarrow \pi^*(mpyz^+)$ bands are observed at especially low energy owing to the strongly π-accepting nature of the $mpyz^+$ ligand. The spectra of the

isomeric pair of complexes in **3** and **17** are somewhat different, with the $d_\pi(Ru^{II}) \rightarrow \pi^*(bpy)$ band maximum occurring at higher energy by ca. 0.19 eV in the *cis* isomer. Besides their MLCT bands, all of the complexes also show one or more intense UV absorptions due to intraligand $\pi \rightarrow \pi^*$ excitations.

3.4. Electrochemical studies

All of the new complex salts were studied by cyclic voltammetry in acetonitrile and results are presented in Table 3. All exhibit reversible or quasi-reversible $Ru^{III/II}$ oxidation waves, together with ligand-based reduction processes which

Table 3
Electrochemical and UV–vis data for complex salts in acetonitrile

Complex salt	$E_{1/2}$ (V vs. SCE) (ΔE_p (mV)) [a]		λ_{max} (nm)	Assignment
	$Ru^{III/II}$	Ligand waves	(ε ($dm^3\ mol^{-1}\ cm^{-1}$)) [b]	
1 *trans*-[RuCl(pdma)(bpy)py]PF_6	0.88 (60)	−1.49 (70)	440sh (4100)	$d\pi \rightarrow \pi^*$(bpy)
			342 (7600)	$d\pi \rightarrow \pi^*$(py)
			296 (21800)	$\pi \rightarrow \pi^*$
			246 (14800)	$\pi \rightarrow \pi^*$
2 *trans*-[RuCl(pdma)(bpy)PPh_3]PF_6	1.29 (60)	−1.30 (170)	398 (4400)	$d\pi \rightarrow \pi^*$(bpy)
			298 (17600)	$\pi \rightarrow \pi^*$
3 *trans*-[RuCl(pdma)(bpy)mim]PF_6	0.68 (70)	−1.54 (90)	458 (3900)	$d\pi \rightarrow \pi^*$(bpy)
			344 (4700)	$\pi \rightarrow \pi^*$
			296 (19400)	$\pi \rightarrow \pi^*$
			248 (12100)	$\pi \rightarrow \pi^*$
4 *trans*-[RuCl(pdma)(bpy)(MeCN)]PF_6	0.96 (60)	−1.53 (70)	430 (4000)	$d\pi \rightarrow \pi^*$(bpy)
			292 (20600)	$\pi \rightarrow \pi^*$
			244 (12400)	$\pi \rightarrow \pi^*$
5 *trans*-[RuCl(pdma)(bpy)dmso]PF_6	1.47 [c]	−1.38 (70)	378 (3900)	$d\pi \rightarrow \pi^*$(bpy)
			292 (14900)	$\pi \rightarrow \pi^*$
			246 (11000)	$\pi \rightarrow \pi^*$
6 *trans*-[RuCl(pdma)(bpy)pyz]PF_6	1.04 (70)		430 (10000)	$d\pi \rightarrow \pi^*$(pyz/bpy)
			294 (25200)	$\pi \rightarrow \pi^*$
			248 (20800)	$\pi \rightarrow \pi^*$
7 *trans*-[RuCl(pdma)(bpy)($mpyz^+$)][PF_6]$_2$	1.29 (90)	−0.48 (80)	572 (20200)	$d\pi \rightarrow \pi^*(mpyz^+)$
		−1.52 [d]	402 (5400)	$d\pi \rightarrow \pi^*$(bpy)
		−1.72 [d]	288 (22900)	$\pi \rightarrow \pi^*$
8 *trans*-[RuCl(pdma)(phen)py]PF_6	0.88 (80)	−1.48 (110)	438 (7400)	$d\pi \rightarrow \pi^*$(phen)
			266 (45200)	$\pi \rightarrow \pi^*$
9 *trans*-[RuCl(pdma)(phen)PPh_3]PF_6	1.28 (80)	−1.24 (60)	398 (4900)	$d\pi \rightarrow \pi^*$(phen)
			268 (35500)	$\pi \rightarrow \pi^*$
10 *trans*-[RuCl(pdma)(phen)mim]PF_6	0.67 (80)	−1.55 (100)	448 (9200)	$d\pi \rightarrow \pi^*$(phen)
			268 (33000)	$\pi \rightarrow \pi^*$
11 *trans*-[RuCl(pdma)(phen)pyz]PF_6	1.02 (90)	−1.42 (130)	410 (6700)	$d\pi \rightarrow \pi^*$(pyz/phen)
			268 (33600)	$\pi \rightarrow \pi^*$
12 *trans*-[RuCl(pdma)(phen)($mpyz^+$)][PF_6]$_2$	1.30 (110)	−0.44 (70)	572 (16900)	$d\pi \rightarrow \pi^*(mpyz^+)$
		−1.37 (170)	394 (5200)	$d\pi \rightarrow \pi^*$(phen)
			268 (36000)	$\pi \rightarrow \pi^*$
13 *trans*-[Ru(pdma)(bpy)$(mim)_2$][PF_6]$_2$	1.06 (110)	−1.36 (80)	412 (3700)	$d\pi \rightarrow \pi^*$(bpy)
			292 (20400)	$\pi \rightarrow \pi^*$
			246 (12400)	$\pi \rightarrow \pi^*$
14 *trans*-[Ru(pdma)(bpy)(mim)py][PF_6]$_2$	1.25 (140)	−1.32 (80)	398 (4400)	$d\pi \rightarrow \pi^*$(bpy)
			288 (20600)	$\pi \rightarrow \pi^*$
			244 (14500)	$\pi \rightarrow \pi^*$
15 *trans*-[Ru(pdma)(bpy)mim(MeCN)][PF_6]$_2$	1.28 (150)	−1.39 (70)	390 (6100)	$d\pi \rightarrow \pi^*$(bpy)
			288 (20700)	$\pi \rightarrow \pi^*$
			246 (14200)	$\pi \rightarrow \pi^*$
16 *trans*-[Ru(pdma)(bpy)PPh_3(MeCN)][PF_6]$_2$	1.82 (120)	−1.23 (50)	364 (6000)	$d\pi \rightarrow \pi^*$(bpy)
			288 (15900)	$\pi \rightarrow \pi^*$
17 *cis*-[RuCl(pdma)(bpy)mim]PF_6	0.67 (80)	−1.56 (80)	428 (6200)	$d\pi \rightarrow \pi^*$(bpy)
			320sh (7700)	$\pi \rightarrow \pi^*$
			290 (24600)	$\pi \rightarrow \pi^*$

[a] Measured in solutions ca. 10^{-3} mol dm^{-3} in analyte and 0.1 mol dm^{-3} in $NBu^n_4PF_6$ at a platinum-bead working electrode with a scan rate of 200 mV s^{-1}. Ferrocene internal reference $E_{1/2} = 0.41$ V, $\Delta E_p = 90$ mV.
[b] Solutions (5–7) $\times 10^{-5}$ mol dm^{-3}.
[c] E_{pa} for an irreversible oxidation process.
[d] E_{pc} for an irreversible reduction process.

range from reversible to irreversible. Within the series *trans*-$[Ru^{II}Cl(pdma)(bpy)L_1][PF_6]_n$ ($n = 1$ or 2, **1**–**7**) the $Ru^{III/II}$ $E_{1/2}$ values become more positive as the overall electron donor strength of L_1 decreases, in the order $L_1 = mim > py > MeCN > pyz > mpyz^+ \approx PPh_3 > dmso$. As expected, this trend parallels that observed in the $d_\pi(Ru^{II}) \rightarrow \pi^*(bpy)$ MLCT data (see earlier). The $Ru^{III/II}$ $E_{1/2}$ values of the phen complexes in **8**–**12** are essentially identical to those of their bpy counterparts, and the same dependence upon L_1 is evident. Similarly, in the disubstituted complex salts *trans*-$[Ru^{II}(pdma)(bpy)mim(L_2)][PF_6]_2$ (**13**–**15**) the $Ru^{III/II}$ $E_{1/2}$ values shift to more positive potentials as the electron donor strength of L_2 decreases in the order $mim > py > MeCN$. The complex in **16** has an especially anodic $Ru^{III/II}$ $E_{1/2}$ due to the combined π-electron-withdrawing abilities of the MeCN and PPh_3 ligands. The cyclic voltammograms of **3** and **17** are essentially identical, showing that isomerization does not affect the redox properties of these complexes.

3.5. Structural studies

Single-crystal X-ray structures were determined for **1**, **2**·DMF, **3**, **12**·3MeCN, **14**·DMF and **17**. Representations of the complex cations are shown in Figs. 1–6. The complexes in **1**, **2**·DMF and **3** show the expected *trans* arrangement of the pdma and bpy ligands. In **2**·DMF, the steric bulk of the PPh_3 causes the pdma and bpy ligands to bend slightly towards the chloride, giving an average E–Ru–Cl (E = As or N) bond angle of 84.25(9)°. The corresponding average bond angles in **1** and **3** are 88.3(1) and 88.7(1)°, respectively, showing very little distortion of the octahedral coordination geometries. The Ru–Cl bond distances increase in the order **1** < **3** < **2**·DMF, with a difference of ca. 0.04 Å between **1** and **2**·DMF. This trend reveals the structural *trans*-effect (STE) order with respect to *trans* chloride of $py < mim < PPh_3$.

The structure of **14**·DMF confirms that the *trans* geometry of **3** is maintained upon substitution of the chloride with a pyridine ligand, and the *trans* structure is also found in **12**·3MeCN. In the latter salt, the Ru–N($mpyz^+$) distance (2.019(2) Å) is ca. 0.1 Å shorter than the average Ru–N(phen) distance, owing to a greater degree of π-back donation to the $mpyz^+$ ligand. The complex in $[Ru^{II}(NH_3)_5(mpyz^+)]I_3$ exhibits a still shorter Ru–N($mpyz^+$) distance (1.95(1) Å) [29], indicating that the presence of the strongly basic ammine ligands gives rise to more extensive $Ru^{II} \rightarrow mpyz^+$ back-bonding than is found in **12**·3MeCN.

The structure of **17** confirms that the isomerization of **3** has taken place, with the chloride ligand now *trans* to a bpy N atom. The cation in **17** is chiral and only one absolute configuration at Ru is found in the crystal. The Ru–Cl bond distance in **17** is ca. 0.01 Å shorter than that in **3**, showing that mim has a slightly larger STE than bpy with respect to chloride. Also, the Ru–N(bpy) bond distances are 2.056(4) Å (*trans* to chloride) and 2.101(4) Å (*trans* to pdma), showing that the pdma ligand exerts a rather greater STE on bpy than does chloride. The Ru–As bond distances of 2.3836(7) Å (*trans* to bpy) and 2.3686(7) Å (*trans* to mim) indicate that the STE of bpy on pdma is slightly larger than that of mim.

4. Conclusion

Stepwise substitutions of the axial nitrosyl and chloride ligands are readily achieved in the mixed-chelates *trans*-$[Ru^{II}Cl(pdma)(L–L)(NO)][PF_6]_2$ (L–L = bpy or phen). However, the resulting products are mildly photosensitive in solution and isomerize irreversibly to their *cis* forms. The preparation of chromophore-quencher complexes based on *trans*-$\{Ru^{II}(pdma)(L–L)\}^{2+}$ centres is therefore unlikely to be a worthwhile objective.

Supplementary data

Supplementary data (fractional atomic coordinates, anisotropic thermal parameters, and full listings of bond lengths and angles) are available from the Cambridge Crystallographic Data Centre, 12 Union Road, Cambridge CB2 1EZ, UK (fax: +44-1223-336033; e-mail: deposit@ccdc.cam.ac.uk) on request, quoting the deposition numbers CCDC 139504 (**1**), CCDC 139505 (**2**·DMF), CCDC 139506 (**3**), CCDC 139507 (**12**·3MeCN), CCDC 139508 (**14**·DMF) and CCDC 139509 (**17**).

Acknowledgements

Thanks are due to the Nuffield Foundation for financial support and to the EPSRC for provision of a studentship (CIM). We are grateful to Johnson Matthey plc for a generous loan of ruthenium trichloride.

References

[1] T.J. Meyer, Acc. Chem. Res. 22 (1989) 163.
[2] V. Balzani, F. Scandola, Supramolecular Photochemistry, Ellis Horwood, Chichester, 1991.
[3] B. O'Regan, M. Grätzel, Nature 353 (1991) 737.
[4] K. Kalyanasundaram, M. Grätzel, Coord. Chem. Rev. 177 (1998) 347.
[5] V. Grosshenny, A. Harriman, M. Hissler, R. Ziessel, Platinum Metals Rev. 40 (1996) 26, 72.
[6] F.R. Keene, Coord. Chem. Rev. 166 (1997) 121.
[7] J.-P. Collin, P. Gaviña, V. Heitz, J.-P. Sauvage, Eur. J. Inorg. Chem. 1 (1998) 1.
[8] B.J. Coe, D.A. Friesen, D.W. Thompson, T.J. Meyer, Inorg. Chem. 35 (1996) 4575.
[9] P.G. Douglas, R.D. Feltham, H.G. Metzger, J. Am. Chem. Soc. 93 (1971) 84.
[10] B.J. Coe, M. Chery, R.L. Beddoes, H. Hope, P.S. White, J. Chem. Soc., Dalton Trans. (1996) 3917.

[11] B.J. Coe, S. Hayat, R.L. Beddoes, M. Helliwell, J.C. Jeffery, S.R. Batten, P.S. White, J. Chem. Soc., Dalton Trans. (1997) 591.
[12] B.J. Coe, C.I. McDonald, R.L. Beddoes, Polyhedron 17 (1998) 1997.
[13] SHELXTL 5.03 program system, Siemens Analytical X-Ray Instruments, Madison, WI, 1995.
[14] R. Hooft, Collect, Data collection software, Nonius BV, Delft, The Netherlands, 1998.
[15] Z. Otwinowski, W. Minor, Methods Enzymol. 276 (1997) 307.
[16] R.H. Blessing, Acta Crystallogr., Sect. A 51 (1995) 33.
[17] R.H. Blessing, J. Appl. Crystallogr. 30 (1997) 421.
[18] S. Mackay, C.J. Gilmore, C. Edwards, M. Tremayne, N. Stewart, K. Shankland, MAXUS, a computer program for the solution and refinement of crystal structures from diffraction data, University of Glasgow, UK, Nonius BV, Delft, The Netherlands and MacScience Co. Ltd., Yokohama, Japan, 1998.
[19] G.M. Sheldrick, Acta Crystallogr., Sect. A 46 (1990) 467.
[20] G.M. Sheldrick, SHELXL 97, Program for crystal structure refinement, University of Göttingen, Germany, 1997.
[21] F. Bottomley, Acc. Chem. Res. 11 (1978) 158.
[22] J.A. McCleverty, Chem. Rev. 79 (1979) 53.
[23] S.A. Adeyemi, E.C. Johnson, F.J. Miller, T.J. Meyer, Inorg. Chem. 12 (1973) 2371.
[24] C.A. Bignozzi, S. Roffia, C. Chiorboli, J. Davila, M.T. Indelli, F. Scandola, Inorg. Chem. 28 (1989) 4350.
[25] B.J. Coe, T.J. Meyer, P.S. White, Inorg. Chem. 34 (1995) 593.
[26] P. Bonneson, J.L. Walsh, W.T. Pennington, A.W. Cordes, B. Durham, Inorg. Chem. 22 (1983) 1761.
[27] P. Ford, F.P. De Rudd, R. Gaunder, H. Taube, J. Am. Chem. Soc. 90 (1968) 1187.
[28] C.R. Johnson, R.E. Shepherd, Inorg. Chem. 22 (1983) 2439.
[29] J.F. Wishart, A. Bino, H. Taube, Inorg. Chem. 25 (1986) 3318.